

# Unravelling Binding Effects in Cyclodextrin Inclusion Complexes with Diamondoid Ammonium Salt Guests

Marija Alešković,<sup>a</sup> Sunčica Roca,<sup>b</sup> Ruža Jozepović,<sup>a</sup> Nikola Bregović,<sup>c\*</sup> Marina Šekutor<sup>a\*</sup>

<sup>a</sup> Department of Organic Chemistry and Biochemistry, Ruđer Bošković Institute, Bijenička 54, 10 000 Zagreb, Croatia, [msekutor@irb.hr](mailto:msekutor@irb.hr)

<sup>b</sup> NMR Center, Ruđer Bošković Institute, Bijenička 54, 10 000 Zagreb, Croatia.

<sup>c</sup> Department of Chemistry, Faculty of Science, University of Zagreb, Horvatovac 102a, 10 000 Zagreb, Croatia, [nbregovic@chem.pmf.hr](mailto:nbregovic@chem.pmf.hr)

**Keywords:** diamondoid ammonium salts, cyclodextrins, host-guest chemistry, thermodynamics

## Abstract

With an ever-growing application of inclusion complexes of cyclodextrins (CDs) and other hydrophobic guests in pharmaceutical industry and other scientific and industrial fields, the demand for deeper understanding of effects defining their stability increases. In this work we investigated the formation of inclusion complexes of diamondoid derivatives containing the ammonium moiety with  $\beta$ - and  $\gamma$ -cyclodextrins using NMR, ITC and conductometric titrations. The adamantane- and diamantane-based guests containing one ammonium group formed stable 1:1 complexes with  $\beta$ -CD, whereas only the diamantane derivative interacted with  $\gamma$ -CD. The thermodynamics of the binding processes was characterized in detail by means of ITC and the origin of the enthalpic and entropic contributions was discussed. Structural features of the complexes were deduced from the data gathered by NOESY NMR and computational studies revealing the key interactions within the inclusion complexes.

Surprisingly, the diammonium derivative did not exhibit any affinity towards inclusion in the cavity of the investigated CDs, which was in strong contrast with its behavior when cucurbituril was used as a host. By providing comprehensive structural and thermodynamic data, this study gives a firm basis for understanding the effects defining the stability of inclusion complexes of charged diamondoid guests with cyclodextrins.

## 1. Introduction

Rational design of efficient host–guest systems has to this day remained one of the fundamental topics in supramolecular chemistry. Implementation of inclusion complexes in catalysis,<sup>1,2</sup> molecular devices,<sup>3</sup> medicine and pharmacy,<sup>4</sup> and other fields closely related to everyday life was for the most part made possible by the ingenious design of diverse supramolecular architectures.<sup>5</sup> Among versatile host scaffolds, cyclodextrins (CDs),<sup>6–9</sup> cucurbit[n]urils (CB[n]),<sup>2,10,11</sup> calixarenes,<sup>12</sup> pillar[n]arenes,<sup>13,14</sup> cyclophanes,<sup>15</sup> and cryptophanes<sup>16</sup> gained the most attention due to their ubiquitous applicability. Common to these classes of hosts is the existence of a deep, centrally positioned cavity, which is a structural feature essential for accommodation of hydrophobic guest molecules *via* their non-polar parts. However, the cavity of the “empty” host is not really empty in any real system, since it interacts with solvent molecules. In the case of aqueous solutions, water molecules populating the cavity of low polarity are somewhat isolated from bulk water molecules and as a consequence cannot be optimally stabilized in such an environment.<sup>17</sup> The release of these high-energy water molecules upon encapsulation of the guest molecule can be responsible for strong affinities, even to the point of being the primary driving force for the complex formation resulting in the high-affinity complexes.<sup>17</sup> Another factor which should be taken into account in the course of the design of an efficient supramolecular host is the size and shape complementarity of its interior and the targeted guest molecule.<sup>18,19</sup> Namely, a good

structural fit enables utilization of the full potential for non-covalent host-guest interactions, while the optimal structural rigidity minimizes the entropic cost of the binding process. Similarly, the suitable geometric features of the host's molecular rim ensure the accessibility of the binding site to the guest molecule. Consequently, these factors play an important role in the design of highly selective and sensitive supramolecular systems.<sup>20</sup>

As part of our ongoing research, we have identified diamondoid derivatives that contain the positively charged ammonium functional group as excellent guest molecules for cucurbituril (CB[n]) hosts in the aqueous environment.<sup>21</sup> In search of the most efficient inclusion interaction, we varied the type, number and position of the amine substituent on the adamantane or diamantane scaffold. The investigation of the resulting inclusion complexes obtained in such a manner enabled us to gain deeper insight in the interplay of various supramolecular effects and to identify which guest characteristics are crucial to afford the strongest binding. We previously found that the 4,9-diammonium diamantane derivative formed an especially stable complex with CB[7], having an attomolar dissociation constant that rivaled even the naturally occurring avidin-biotin interaction.<sup>21b</sup> When compared to an aromatic guest with a scaffold of similar dimensions and functional group placement,<sup>22</sup> it was shown that the bulky diamantane cage more effectively pushed out the high-energy water molecules from the cavity interior, thus highlighting the connection between a good structural fit and efficient solvent extrusion. Moreover, while the guest scaffold was perfectly accommodated into the cavity, its amine substituents established a harmonious interaction with both rims of CB[7]. By identifying the key features responsible for strong host-guest binding of diamondoid guests, we could next embark on a rational design of the next generation of inclusion complexes, using different macrocycles, *i.e.*, cyclodextrins (CDs). Many literature examples exist detailing inclusion complexes of lipophilic adamantane derivatives with  $\beta$ -CDs,<sup>23-29</sup> but only a few examples describe the binding of larger

diamondoid homologues into a  $\beta$ - or especially  $\gamma$ -CD cavity, which is bigger and more flexible.<sup>30</sup> One such recent report deals with adamantane, diamantane and triamantane amines, carboxylic acids and its derivatives as suitable guests for  $\beta$ - and  $\gamma$ -CDs.<sup>30</sup> The authors presented a comprehensive thermodynamic study and showed that 1:1 adamantane derivative complexes with  $\beta$ -CD achieved typical association constants of about  $10^4 \text{ mol}^{-1} \text{ dm}^3$ . On the other hand, diamantane and triamantane derivatives showed the strongest binding affinities towards  $\beta$ - and  $\gamma$ -CDs (association constants  $>10^5 \text{ mol}^{-1} \text{ dm}^3$ ) reported so far for this class of compounds. In addition, it was proposed that triamantane formed 1:2 complexes with  $\beta$ -CD.<sup>30b</sup>

Herein we present the study of inclusion phenomena between diamondoid ammonium salts **1–3** and  $\beta$ - and  $\gamma$ -CD hosts (Figure 1). We used ITC, conductometric and  $^1\text{H}$  NMR titrations to assess the binding strength, as well as additional NMR spectroscopic techniques to gain insight into the structural properties of the studied complexes. Our experimental findings were additionally supported by a computational study of the formed inclusion complexes. The binding capability was discussed taking into account the size of the molecular scaffold and the number of substituents, as well as the cyclodextrin cavity size.

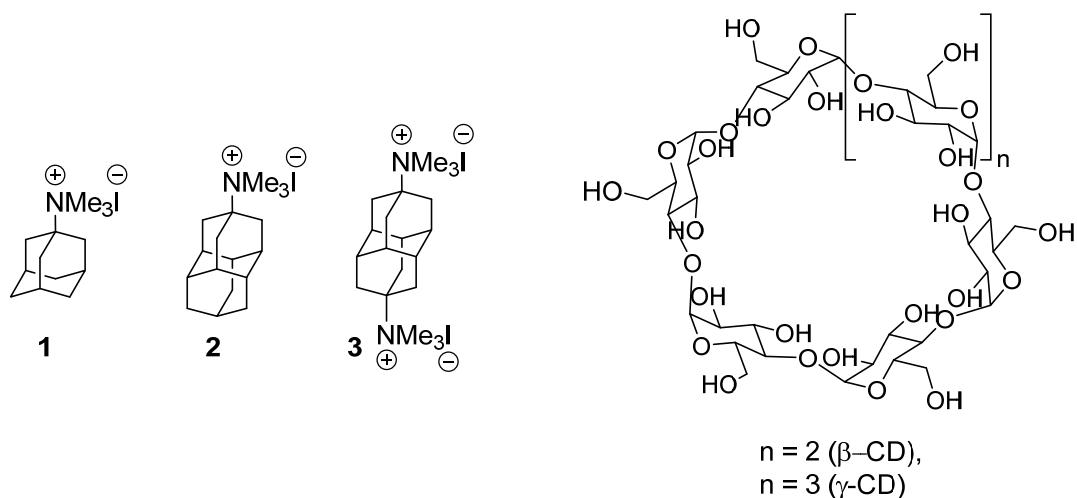
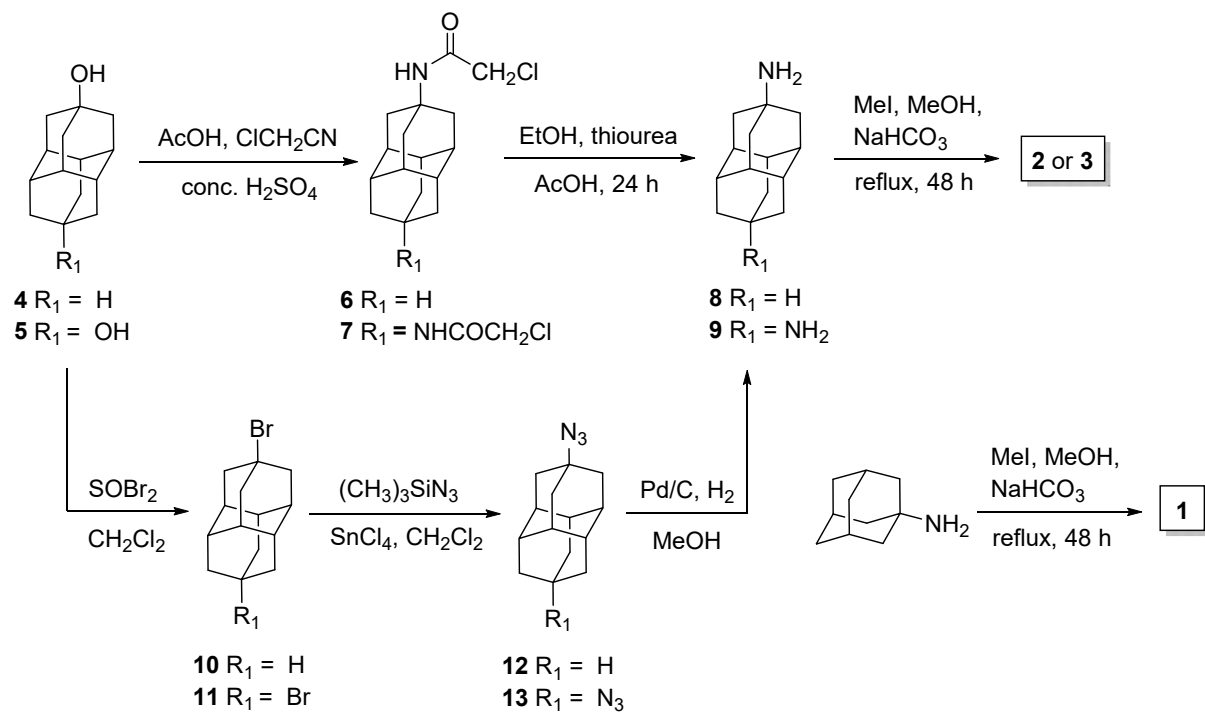


**Figure 1.** Structures of diamondoid ammonium salt guests **1–3** and cyclodextrin hosts ( $\beta$ - and  $\gamma$ -CD).

## 2. Results and Discussion

The key step in the synthesis of permethylated diamantane ammonium salts **1–3** was selective functionalization of the diamantane scaffold *via* nitroxylation and subsequent hydrolysis to the corresponding alcohols, as was previously described in the literature.<sup>31</sup> After chromatographic separation of the obtained alcohol mixture and isolation of pure alcohols **4** and **5**, two synthetic approaches were considered (Scheme 1). The first pathway included acid-catalyzed reaction of the respective diamondoid alcohol with chloroacetonitrile to afford compounds **6** and **7**, which were cleaved without isolation using thiourea to produce diamondoid amines **8** and **9**, respectively.<sup>32</sup>



**Scheme 1.** Preparation of permethylated guest molecules **1–3**.<sup>21,31–34</sup>

The alternative synthesis of the required amine precursors was accomplished by using thionyl bromide to convert alcohol derivatives **4** and **5** to bromides **10** and **11**, respectively. The bromides then underwent azidation to afford azides **12** and **13**, which were subsequently

reduced with the excess of Pd/C to final amines **8** and **9**.<sup>33</sup> Although the first synthetic approach has the advantages of using milder reaction conditions (no thionyl bromide or strong Lewis acids like  $\text{SnCl}_4$ ), its main drawback is a somewhat tedious purification of amines from the thiourea reaction byproducts. All afforded amines, including the commercially available adamantane amine, were converted to target salts **1–3** after exhaustive permethylation.<sup>21,22,34</sup> After preparing target molecules **1–3**, we determined equilibrium constants and other thermodynamic parameters for the complexation of **1–3** with CDs and our findings are compiled in Table 1.

**Table 1.** Thermodynamic parameters and association constants of the complexes of **1–3** with CDs determined by ITC, conductometry and  $^1\text{H}$  NMR titrations.<sup>a</sup>

| Host         | Guest    | logK             |                  |                            | $\Delta_fH^\circ /$<br>$\text{kJ mol}^{-1}$ | $\Delta_rS^\circ /$<br>$\text{J K}^{-1} \text{mol}^{-1}$ | $\Delta A /$<br>$\text{S cm}^2 \text{mol}^{-1}$ |
|--------------|----------|------------------|------------------|----------------------------|---|--|---|
|              |          | ITC <sup>b</sup> | NMR <sup>c</sup> | Conductometry <sup>c</sup> |   |  |   |
| $\beta$ -CD  | <b>1</b> | 3.725(3)         | 3.8(1)           | 3.61(1)                    | -25.6(4)                                    | -15(1)   | -17.1   |
|              | <b>2</b> | 4.98(1)          | > 4              | $\approx 5^d$              | -33.6(4)                                    | -17(1)   | -14   |
| $\gamma$ -CD | <b>1</b> | no binding       |                  |                            |   |  |   |
|              | <b>2</b> | -                | 3.37             | 3.52(1)                    |   | -  | -7.1  |

Thermodynamic data obtained at the operating temperature of 25.0 °C. <sup>a</sup> No binding of **3** with CDs was observed. <sup>b</sup> The uncertainties are given in parentheses as standard error of the mean ( $N = 3$ ). <sup>c</sup> The uncertainties are given in parentheses as standard deviation. <sup>d</sup> Estimated value.

The affinities of cyclodextrins to form host–guest complex with the prepared derivatives of adamantane (**1**) and diamantane (**2**) in aqueous solution were investigated by means of ITC and conductometric titrations. The titration curves obtained by both methods could be processed by assuming the formation of a 1:1 complex, confirming that this is indeed the only complex formed. The complexes of studied diamantane derivative with  $\beta$ -CD exhibited the highest stability with logK value just short of 5. This indicated that the  $\beta$ -CD cavity provided a good fit for the diamantane derivative. The investigated adamantane derivative exhibited

substantial affinity for inclusion in  $\beta$ -CD ( $\log K = 3.725$ ) but still significantly lower compared to complexation of **2** with this host. On the other hand, no significant heat signals were detected upon addition of  $\gamma$ -CD to the solution of adamantane derivative **1**, suggesting that this guest did not interact with  $\gamma$ -CD. The ITC titration curve obtained by addition of  $\gamma$ -CD to the solution **2** could not be fitted by applying any reasonable model.

The ITC experiments provided additional information about enthalpic and entropic contribution to the standard reaction Gibbs for complex formation. In all cases it was found that the complexation is an exothermic process with a negative standard entropy change. The favorable enthalpic effect of the inclusion originated from the release of the high-energy water molecules extruded from the CD cavity upon the inclusion of the guests. On the other hand, the unfavorable entropic effect could be ascribed to the loss in translational and rotational entropy of the host and guest upon complex formation. The stability of the complexes could be correlated to the size compatibility of the hosts **1** and **2** and the studied cyclodextrins. Since the studied guests are positively charged, we could apply conductometry as an additional method for the study of their interactions with cyclodextrins. Namely, the complex was expected to feature significantly lower molar conductivities (mobililities) compared to free **1** or **2** due to the increased size. This was indeed the case and a drop in the solution conductivity upon addition of CDs to the solutions of **1** or **2** was detected. The conductometric titration curves ( $\kappa$  vs.  $c(\text{CD})$ ) could again be processed by assuming only the 1:1 complex stoichiometry and the calculated stability constants were in good agreement with those determined by ITC (and  $^1\text{H}$  NMR) titrations, further confirming our findings. As stated above, the results of microcalorimetric titration regarding **2** and  $\gamma$ -CD could not be reliably interpreted. In contrast, conductometric titration was found to be a suitable method to investigate the system in question. The obtained titration curve provided clear information on the stoichiometry of the complex between **2** and  $\gamma$ -CD (again 1:1) and afforded the related

stability constant, which was in line with the value obtained by NMR (Table 1). Note that the change in the conductivity detected during the titration of adamantane derivative **1** with  $\gamma$ -CD was negligible, again confirming that the complex formation does not occur.

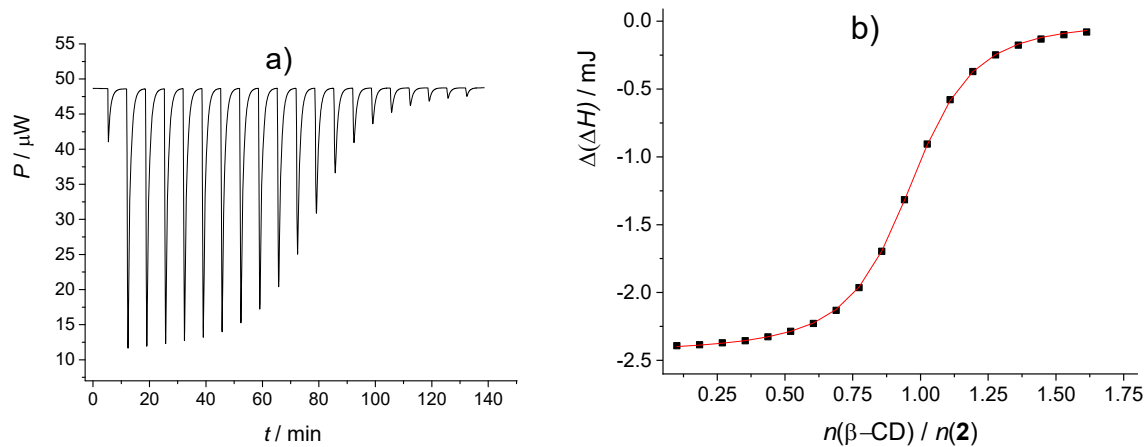


**Figure 2.** a) Microcalorimetric titration of **2** ( $c = 5.9 \times 10^{-4} \text{ mol dm}^{-3}$ ,  $V = 1.425 \text{ mL}$ ) with  $\beta$ -CD ( $c = 4.80 \times 10^{-3} \text{ mol dm}^{-3}$ ) in water at  $25.0 \text{ }^\circ\text{C}$ ; b) Dependence of successive enthalpy change on  $\beta$ -CD to **2** molar ratio; ▀ measured, — calculated.

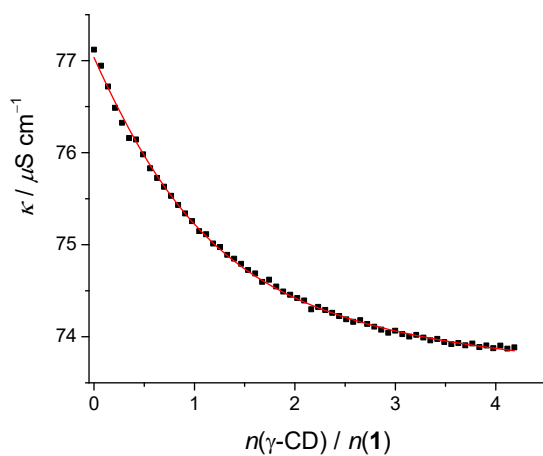


**Figure 3.** Conductometric titration of **2** ( $c = 5.4 \times 10^{-3} \text{ mol dm}^{-3}$ ,  $V_0 = 15 \text{ mL}$ ) with  $\gamma$ -CD ( $c_0 = 0.0113 \text{ mol dm}^{-3}$ ); ▀ measured, — calculated.

All  $^1\text{H}$  NMR titrations of **1–3** with  $\beta$ - and  $\gamma$ -CD were performed in  $\text{D}_2\text{O}$  (see Supplementary Information, Figures S4–S9) and a titration of **2** with  $\gamma$ -CD is shown in Figure 4 as an example. All proton signals of the diamantane scaffold show a downfield shift from 0.02 to 0.09 ppm in the  $^1\text{H}$  spectra after addition of  $\gamma$ -CD host molecules (Figure 4). The change was the most pronounced for the methyl group ( $\Delta\delta = 0.09$  ppm) and the H-2 atom signal ( $\Delta\delta = 0.06$  ppm). Significant upfield (H-2, H-4) and downfield (H-3, H-5) chemical shifts of the  $\gamma$ -CD proton signals were observed as well. The changes obtained for protons H-3 and H-5 from the macrocyclic interior, which were indicative for the guest inclusion, were very similar ( $\Delta\delta = 0.05$  ppm). The shielding of the H-2 and H-4 atom signals was reduced by inclusion ( $\Delta\delta(\text{H-2}) = -0.015$  ppm;  $\Delta\delta(\text{H-4}) = -0.002$  ppm). The described spectral changes observed upon titration of diamondoid amines with CDs were in accordance with the literature data.<sup>23–30</sup> In order to determine the association constant for the inclusion complex **2@ $\gamma$ -CD**, we fitted the dependence of the chemical shifts for multiple signals of the guest on the CDs concentration using the HYPNMR program.<sup>35</sup> The obtained data are summarized in Table 1 as well.

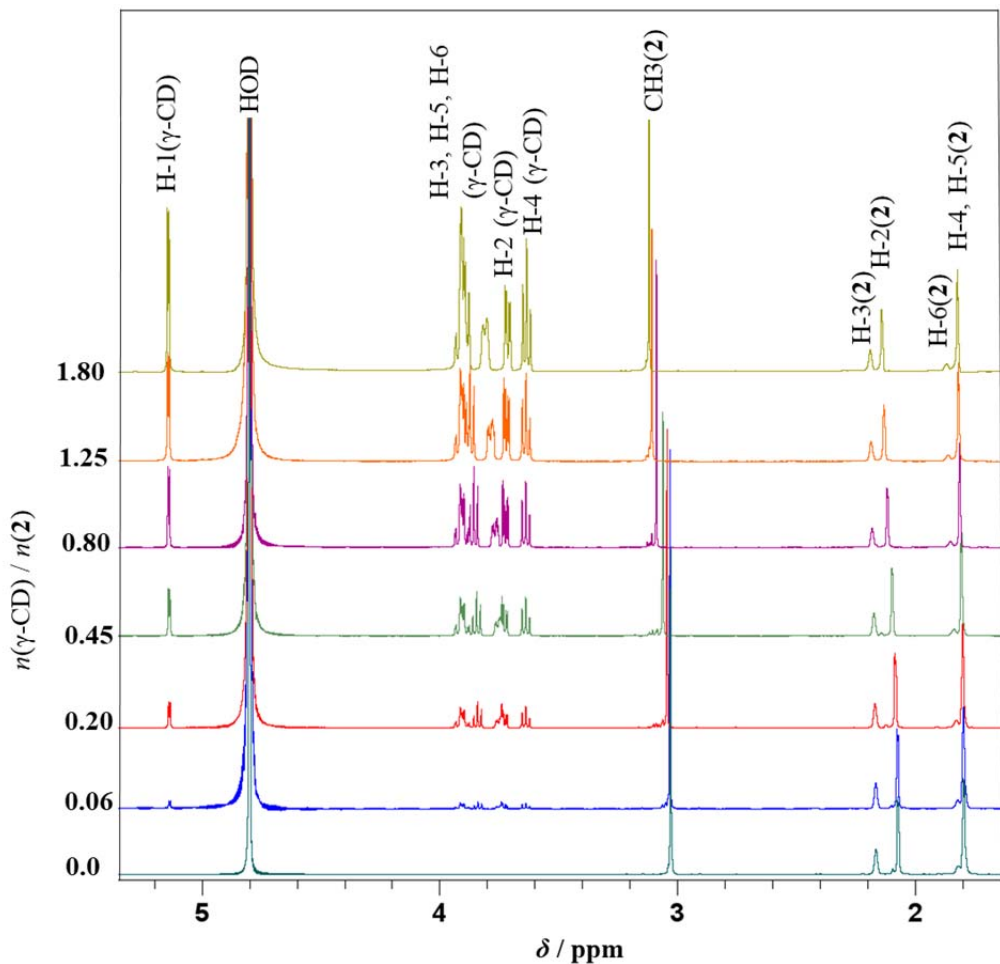


**Figure 4.** Selected  $^1\text{H}$  NMR spectra (600 MHz, 25 °C) obtained by titration of **2** ( $c = 5 \times 10^{-3}$  mol dm $^{-3}$ , bottom spectra) with added equivalents of  $\gamma$ -CD in  $\text{D}_2\text{O}$  (to the top). All  $^1\text{H}$  NMR spectra are shown in Figure S8 in the Supplementary Information.

The changes of the chemical shifts in the  $^1\text{H}$  NMR spectra of host **2** detected upon complexation with  $\beta$ -CD were similar to those recorded when **2** interacted with  $\gamma$ -CD. This suggested that the structural features of both complexes are analogous, *i.e.*, that the inclusion of the host into the cavity of both CDs occurred. The collected titration curve featured a sharp break obtained at 1:1  $\beta$ -CD to **2** molar ratio, which confirmed the complex stoichiometry. However, quantitative characterization of complex formation based on NMR titration data was not possible since the related  $\log K$  was above the limit for reliable determination at the

experimental conditions applied ( $\log K > 4$ ) This is in line with the previously described results obtained by ITC (Table 1), which did provide a reliable value of  $\log K$  to values above 4, which is in turn in line with the conductometric results.

Similarly,  $^1\text{H}$  NMR titrations of **1** and  $\beta$ -CD revealed formation of the inclusion complex with the association constants  $\approx 10^3 \text{ mol}^{-1} \text{ dm}^3$ , while the  $\gamma$ -CD cavity was too large to fit the adamantyl derivative and thus no changes were observed during the titrations. As it has been known from the literature that the adamantane scaffold fits more snugly into the smaller  $\beta$ -CD cavity and binds much more loosely with the  $\gamma$ -CDs,<sup>23-29</sup> our use of a larger diamondoid cage for host encapsulation studies with  $\gamma$ -CD cavity was indeed a valid choice.<sup>30</sup> Binding of bis-apically substituted derivative **3** into the cavities of either host under study was not detected, with neither NMR nor ITC methods. In order to exclude the possibility of slow kinetics of the inclusion, we recorded  $^1\text{H}$  NMR spectra of the solution containing **3** and the studied hosts periodically for a few months. No change in the spectra occurred during this time, thus ruling out a slow exchange. It is curious to note that derivative **3**, which showed such excellent binding with the CB[7] host<sup>21</sup> failed to repeat similar affinity to interact with the CD host family.

In order to gain a deeper insight in the structural characteristics of the inclusion complexes and the interactions affording their stabilization, we performed a  $^1\text{H}$ - $^1\text{H}$  NOESY (Nuclear Overhauser Effect Spectroscopy) experiment. Observed NOE cross peaks between **1** or **2** (H-3, H-5, H-6) and CDs (H-3, H-5, H-6) unequivocally confirmed the insertion of the studied host molecules deep into the CDs cavities (Figure 5).

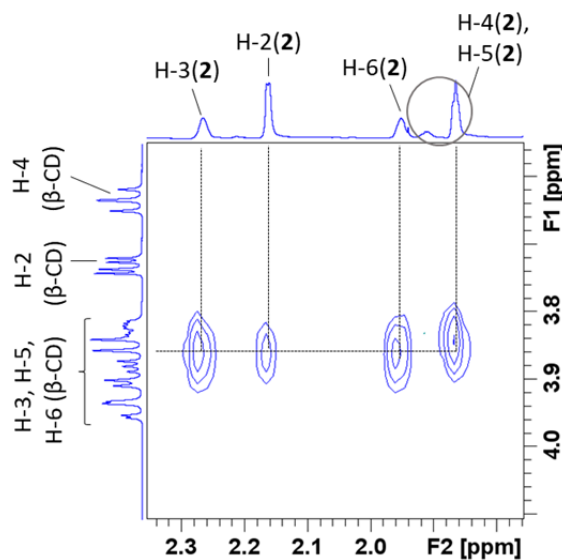


**Figure 5.** NOESY NMR spectrum of **2** with  $\beta$ -CD ( $D_2O$ ,  $25\text{ }^{\circ}\text{C}$ ). The  $600\text{ }{\text{MHz}}$   $^1\text{H}$  NMR spectrum of **2@** $\beta$ -CD is shown at the top and left-hand edges, with assignments.

Complex formation was also corroborated by  $^1\text{H}$  DOSY (Diffusion Ordered Spectroscopy) NMR techniques (Figure 6). The measured diffusion coefficients ( $D / \text{m}^2 \text{ s}^{-1}$ , Table 2) revealed the appearance of host–guest interactions shortly after compounds mixing (see Supplementary Information, Figures S10–S12). The diffusion coefficients of the larger CD molecules remained the same and those of **1** and **2** approached the diffusion coefficient of CDs, which is expected for inclusion complexes. Namely, diffusion coefficient of the supramolecular complex is expected to be approximately the same as that of the host since the guest is included in its cavity, thus not affecting significantly the effective hydrodynamic radius of the complex (Table 2, Figure 6). The  $D$  value for guests in the presence of hosts remained somewhat higher compared to the CD host, due to the fact that equilibrium between the free and the bound form of the guest is established. Therefore, this is more significant in the case of weaker complexes (**1@** $\beta$ -CD and **2@** $\gamma$ -CD). In contrast, in the solution containing  $\gamma$ -CD and **1** the diffusion coefficients of both molecules remained practically the same, as

those determined for the free molecules, again confirming that no complexation between these two compounds takes place.

**Table 2.** Diffusion coefficients ( $D / \text{m}^2 \text{ s}^{-1}$ ) of the studied samples obtained with convection compensation at 14.1 T and 25 °C.<sup>a,b</sup>

| Species                          | Diffusion coefficient $\times 10^{-10} (\text{m}^2 \text{ s}^{-1})$ |                      |
|----------------------------------|---|----------------------|
|                                  | $D_{\text{guest}}$  | $D_{\text{CD}}$      |
| $\beta\text{-CD}_{\text{free}}$  | /   | 3.41 ( $\pm 0.080$ ) |
| $\gamma\text{-CD}_{\text{free}}$ | /   | 3.32 ( $\pm 0.065$ ) |
| <b>1</b> <sub>free</sub>         | 7.89 ( $\pm 0.055$ )  | /                    |
| <b>2</b> <sub>free</sub>         | 7.41 ( $\pm 0.085$ )  | /                    |
| <b>1</b> @ $\beta\text{-CD}$     | 4.89 ( $\pm 0.155$ )  | 3.36 ( $\pm 0.010$ ) |
| <b>2</b> @ $\beta\text{-CD}$     | 3.68 ( $\pm 0.102$ )  | 3.29 ( $\pm 0.105$ ) |
| <b>1</b> @ $\gamma\text{-CD}$    | 7.23 ( $\pm 0.185$ )  | 3.25 ( $\pm 0.022$ ) |
| <b>2</b> @ $\gamma\text{-CD}$    | 4.64 ( $\pm 0.050$ )  | 3.18 ( $\pm 0.065$ ) |

<sup>a</sup>  $c$  of all samples was  $6.0 \times 10^{-3} \text{ mol dm}^{-3}$ . <sup>b</sup> Standard deviations are given in parentheses.

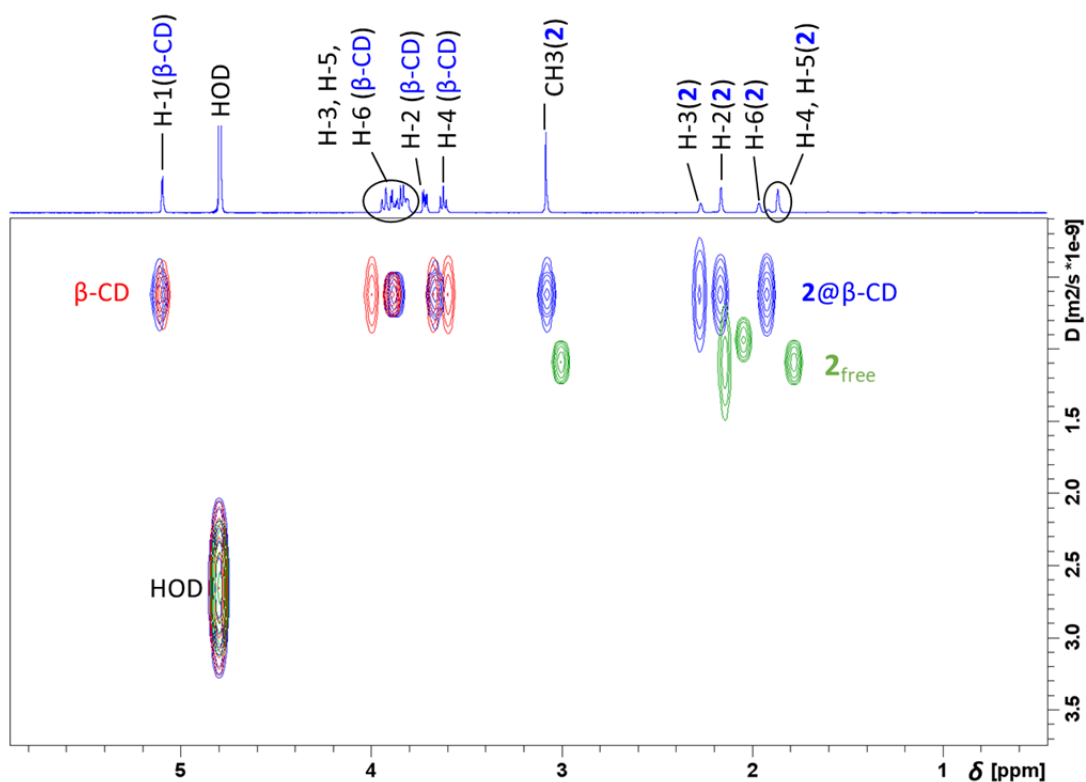


**Figure 6.**  $^1\text{H}$  DOSY NMR spectrum ( $\text{D}_2\text{O}$ , 25 °C) of **2** with  $\beta$ -CD. The 600 MHz  $^1\text{H}$  NMR spectrum of **2@** $\beta$ -CD is shown at the top.

With the aim to further describe and visualize the key interactions stabilizing the inclusion complexes under study and round up our analysis, we also performed DFT optimizations of the host-guest systems using the B3LYP-D3(BJ)/6-31G level of theory with included implicit solvent effects of the water medium by applying the CPCM polarizable conductor calculation model. Using the **2@** $\beta$ -CD complex as an example (depicted on Figure 7), it can be illustrated that the apically substituted permethylated amine **2** undergoes inclusion inside the host cavity primarily by its hydrophobic cage subunit. The resulting complex is further stabilized (locked in) with polar interactions present between the CD rim and the methyl groups of the amine subunit. Also note that a slight tilt of the guest scaffold is observed, which suggests the presence of a pull effect on the host geometry that is dependent on the cage size situated in the central cavity. This host deformation effect expands all the way up to the upper rim of the CD where it slightly disrupts the hydrogen bonding pattern present in the starting host geometry. The computed complex geometry is thus in line with the information gleaned from cross peaks observed in the NOESY spectrum (Figure 5) and supports our starting hypothesis that **2** is deeply immersed in the hydrophobic CD cavity *via* a cage subunit. Analogous depictions of inclusion complexes with other studied guests and  $\beta$ - and  $\gamma$ -CD hosts, that follow a similar binding pattern, are provided in the Supplementary Information.

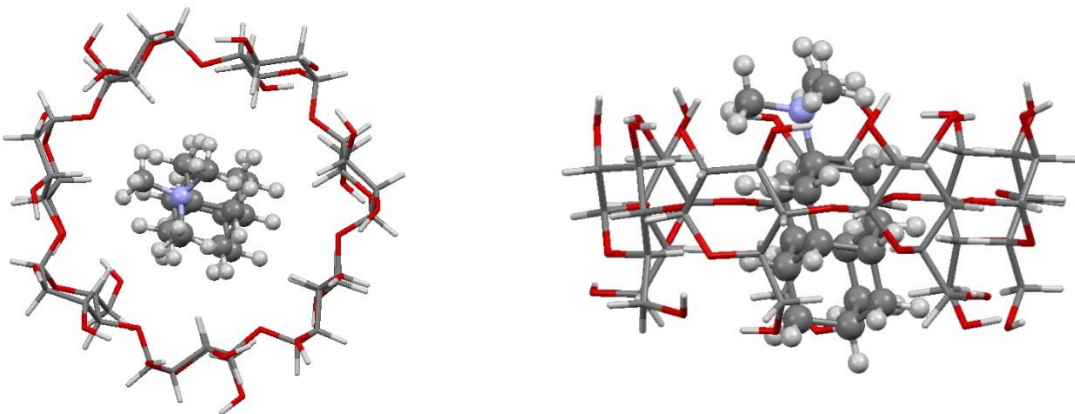


**Figure 7.** Top (left) and side view (right) of the **2**@ $\beta$ -CD complex computed at the CPCM(water)/B3LYP-D3(BJ)/6-31G level of theory.

Our thorough approach to the analysis of inclusion capabilities of charged diamondoid ammonium salts when interacting with the CD host family revealed important trends to consider in efficient guest design. Not only is the cage size (adamantane *vs.* diamantane) a significant factor for achieving a good supramolecular fit, but the effect of the charged functional groups is critical for achieving a successful binding event. What is more, this functional group effect is more pronounced and completely opposite to our previously found trend valid for the CB[n] host family! Namely, complexes of CB[n] hosts with diamondoid ammonium salts possessing two charged groups are remarkably stable and the binding of the guest proceeds with both host portals taking part and, consequently, both ammonium groups are actively engaged in the respective interaction.<sup>21</sup> However, in case of the CD host family such dual binding mode is not favorable at all, to the extent that it even fails to produce detectable complexes. For example, a bis-apical derivative **3**, a record holder in binding with CB[7] in water, performed poorly with both  $\beta$ - and  $\gamma$ -CD, with no measurable affinity for interaction whatsoever. The reason for this stark difference cannot be due to incompatible host-guest size fit since both host families are similar in that regard and what is more, a similarly sized guest **2** produces analogous inclusion complexes with CDs without issues. We

can therefore conclude that the reason for our observation must be due to the presence of a second permethylated ammonium group. A possible explanation for this phenomenon could be that the inclusion of **3** requires a significant unfavorable desolvation of the second positively charged ammonium group during its advancement through the CD's hydrophobic cavity, which could not be overcome by the emerging stabilizing hydrophobic interactions of the CD wall with the diamondoid cage. An argument for that reasoning could be made by considering the general binding strengths of diamondoid ammonium salts with CB[n]s *vs.* CDs. As the binding efficiency of this class of guests with CDs is significantly weaker (of several orders of magnitude), it is not unreasonable to assume that the supramolecular system simply cannot compensate for the excessively unfavorable desolvation of the polar group that would need to push through the CD cavity to reach the other rim if a complex were to form. It is also possible that the rate of the inclusion process of **3** is extremely low, concealing the thermodynamic stability of the resulting complex, *i.e.*, that the process is kinetically controlled. In this case, the guest again needs to penetrate the guest cavity with its hydrophilic charged part in order to achieve the favorable hydrophobic contacts in the end. The system thus needs to cross a highly unfavorable transition state which could result in a high energy barrier, meaning that the complexation reaction would be slowed down significantly. A support for this reasoning can also be found in the literature by considering the binding of a structurally analogous derivative, 4,9-diaminodiamantane, with CDs.<sup>30b</sup> Namely, the authors of the study noted that this bis-apical amine engaged in weak interactions with both  $\beta$ - and  $\gamma$ -CD and reasoned that the dicationic character of the molecule makes it a perfect guest for CB[7] that has polar portals but on the other hand makes it unsuitable for CDs due to disruptive interactions with the hydrophobic CD cavity. It is therefore gratifying to confirm that the interaction pattern previously found for the dicationic cage ammonium derivative also holds true for the trimethylammonium guest investigated herein. Overall, our findings

demonstrate an important point: hosts with hydrophobic cavities of similar geometric features can act in a completely different manner if their structural stiffness and electrostatic properties are altered, especially when charged guests are considered, which has important implications for the inclusion complexes design in general.

## Conclusions

A series of permethylated ammonium diamondoid salts was prepared and their inclusion complexes with  $\beta$ - and  $\gamma$ -cyclodextrin hosts in water were investigated in detail from a thermodynamic and a structural point of view. Equilibrium constants and other thermodynamic parameters for the complexation of studied guests with CDs were determined by isothermal titration calorimetry (ITC), conductometric and  $^1\text{H}$  NMR titrations.

Both mono-ammonium derivatives **1** and **2** were efficiently included in  $\beta$ -cyclodextrin with the complexation reaction enthalpically driven and entropically unfavorable. Diamantane-based guest **2** also interacted with  $\gamma$ -cyclodextrin and formed complexes of 1:1 stoichiometry, which was deduced from NMR and conductometric titrations. DOSY NMR experiments provided further proof of inclusion since the measured diffusion coefficient for **1** or **2** in the presence of a CD approached the one of the host.  $^1\text{H}$ - $^1\text{H}$  NOESY NMR spectroscopy along with the corresponding computational analysis were employed to elucidate specific interactions between the CD hosts and the encapsulated diamondoid guest. It was proven that the studied guests entered deep inside the CD cavity, establishing numerous hydrophobic contacts and interacting with the polar host rim *via* the polarized methyl groups of the ammonium moiety.

No interactions between **1** and  $\gamma$ -CD were detected by any of the applied methods, which was due to a poor structural compatibility of this host-guest pair. Furthermore, the introduction of a second apical ammonium group in the diamantane cage structure had a

detrimental effect on the inclusion in the investigated CDs. This intriguing contrast to the interaction of **3** with cucurbit[7]uril (which was previously found to be highly favorable) was rationalized by possibly more demanding desolvation of the guest and its weaker overall interactions with the host.

With the aim of gaining deeper insight in the effects governing the inclusion behavior of positively charged diamondoids and CDs, further modifications of the guest structures will be performed and the corresponding complexes will be studied in various conditions as a continuation of our work.

## Experimental

**Materials and Methods:** All NMR experiments were performed in deuterated water ( $D_2O$ ) at 25 °C using Bruker AV600 NMR spectrometer equipped with the 5 mm diameter observed probe with  $z$ -gradient accessory at the Ruđer Bošković Institute. The chemical shifts ( $\delta$ /ppm) in the  $^1H$  spectra were referred to the  $D_2O$  signal ( $^1H$ :  $\delta$  = 4.80 ppm), and in the  $^{13}C$  spectra to the 1,4-dioxane- $d_8$  as external standard ( $^{13}C$ :  $\delta$  = 66.7 ppm). The  $^1H$  and  $^{13}C$  signal assignments of the final *N*-methylated products **1–3** were confirmed by cross peaks obtained in 2D spectra of  $^1H$ - $^1H$  Correlation Spectroscopy (COSY),  $^1H$ - $^{13}C$  Heteronuclear Multiple Quantum Coherence (HMQC) and  $^1H$ - $^{13}C$  Heteronuclear Multiple Bond Correlation (HMBC). Detailed NMR spectral assignment of guests **1–3** is given in the Supplementary Information (part of Figures S1–3). Host-guest binding was investigated by  $^1H$ - $^1H$  Nuclear Overhauser Effect Spectroscopy (NOESY) and  $^1H$  Diffusion-ordered NMR Spectroscopy (DOSY).

$^1H$  NMR DOSY spectra were acquired using dstebpgp3s pulse sequence with convection compensation. The measuring conditions were as follows: 16 scans, 12.0 kHz sweep width, 16K time domain, 1000  $\mu$ s spoil gradients, 200  $\mu$ s gradient recovery, 2.0 s relaxation delay and 5 ms eddy current delays. The gradient strength was varied from 2% to 95% in 16 steps,

while the little (5.6 ms) and the big (42.0 ms) delta were kept constant. Used spectrometer is equipped with a *z*-gradient system which allows a maximum gradient, *g*, of 58.0 G cm<sup>-1</sup>. The spectra were processed by applying Dynamics Center 2.7.4 software by Bruker Biospin GmbH, Germany. Diffusion coefficients (*D*) were estimated by fitting peak intensities using the function in Equation 1 where  $\gamma$  is 26752 rad/(G s). Note that the HOD signal was used as a reference value, with a diffusion coefficient of about 2.40 m<sup>2</sup> s<sup>-1</sup>.

$$f(x) = Ae^{-Dx^2\gamma^2\delta^2(\Delta-\frac{\delta}{3})} \times 10^4 \quad [1]$$

During the compound synthesis, GC-MS analyses were performed on an Agilent 7890B/5977B GC/MSD instrument equipped with a HP-5MS column. Silica gel (0.05–0.2 mm) was used for chromatographic purifications. Chemicals were purchased from the usual commercial sources and were used as received. Cyclodextrin hosts were purchased from Alfa Aesar ( $\beta$ -CD, M=1162.01 g mol<sup>-1</sup>) and Merck ( $\gamma$ -CD, M=1297.12 g mol<sup>-1</sup>) companies. Solvents for chromatographic separations were used as delivered from the supplier (p.a. or HPLC grade) or purified by distillation (CH<sub>2</sub>Cl<sub>2</sub>). Dry CH<sub>2</sub>Cl<sub>2</sub> was obtained after standing of commercial product over anhydrous MgSO<sub>4</sub> overnight, then filtered and stored over 4 Å molecular sieves. Dry methanol was obtained by standard Mg-methoxide method and stored over 3 Å molecular sieves.

**General procedure for permethylation reaction:** A mixture of amine (1 eq), excess CH<sub>3</sub>I (7.5 eq) and NaHCO<sub>3</sub> (5.0 eq) in methanol (15 mL) was heated to reflux for 48 h. The mixture was cooled, the solvent evaporated and the crude product washed with hot acetone to afford the target solid product (compounds **1–3**, respectively).<sup>21,22,34</sup>

**NMR titrations experiments:** <sup>1</sup>H NMR titrations were performed in a D<sub>2</sub>O solution, *c*(guest) was typically  $5 \times 10^{-3}$  mol dm<sup>-3</sup>. The hosts were added in the concentrations ranging from  $5 \times 10^{-4}$  to  $10^{-2}$  mol dm<sup>-3</sup> (appropriate weights of  $\beta$ -CD or aliquots of  $\gamma$ -CD solution), reaching

the maximal ratio of host:guest = 4:1. After each addition a  $^1\text{H}$  NMR spectrum was recorded at 25 °C. The titration data were fitted to a 1:1 stoichiometry and the association constants were determined using the HYPNMR program.<sup>35</sup>

**ITC experiments:** ITC measurements were performed by means of isothermal titration microcalorimeters (Microcal VP-ITC) at 25.0 °C. Origin 7.0 software, supplied by the manufacturer, was used for the data acquisition and manipulation. The calorimeter was calibrated electrically. Four different calorimeters of the same type were used throughout the research and the volumes of the calorimeter cells were 1.4182 mL, 1.4265 mL, 1.4250 mL, or 1.4497 mL, while the total volume of the burette was 0.3 mL. The ITC titrations were carried out by stepwise addition of aqueous solution of  $\beta$ -CD or  $\gamma$ -CD ( $V_{\text{addition}} = 10$ , or 15  $\mu\text{L}$ ,  $c_0 \approx 5 \times 10^{-3}$  mol dm $^{-3}$ ) to a solution of the prepared adamantane and diamantane derivatives ( $c_0 \approx 5 \times 10^{-4}$  mol dm $^{-3}$ ). Constant stirring was applied, and the time between additions was set to 400 s. In the case of titration of **2** with  $\gamma$ -CD the titration was also performed at higher concentrations of both host and guest ( $c_0(\mathbf{2}) = 4.95 \times 10^{-3}$  mol dm $^{-3}$ ,  $c_0(\gamma\text{-CD}) = 4.7 \times 10^{-2}$  mol dm $^{-3}$ ) due to low heat signals at lower concentration range. Blank experiments were carried out with each titrant solution to obtain heats of dilution. These heats were subtracted from those measured in the titration experiments. The dependence of the measured enthalpy change on the volume of the added titrant was processed by a non-linear least-squares fitting procedure by using the Origin-Pro 7.5 program. In the fitting procedure a model was applied involving only 1:1 complex stoichiometry. All ITC titrations were repeated at least three times and mean values of the determined thermodynamic parameters are given, with uncertainties expressed as standard errors of the mean.

**Conductometric experiments:** Conductometric titrations were performed by stepwise addition of aqueous cyclodextrin solution ( $c(\beta\text{-CD}) \approx 5 \times 10^{-3}$  mol dm $^{-3}$ ,  $c(\gamma\text{-CD}) \approx 1 \times 10^{-2}$  mol dm $^{-3}$ ) to 15 mL solutions of adamantane or diamantane ( $c \approx 7 \times 10^{-4}$  mol dm $^{-3}$ )

derivatives in MiliQ water. The measured solution was constantly stirred using magnetic stirrer. The titrant solutions were added ( $V_{\text{addition}} = 20 \mu\text{L}$ ) using a Hamilton ML500 titrator operated *via* the Hamilton Microlab program. The conductivity of the solution was measured by means of MettlerToledo InLab 741-ISM conductivity cell ( $K_{\text{cell}} = 0.09806 \text{ cm}^{-1}$ ) calibrated with a standard KCl solution (Merck,  $\kappa = 1.413 \text{ mS cm}^{-1}$ ) connected to a MettlerToledo SevenExcellence measuring device. Conductivity data were collected automatically *via* MettlerToledo EasyDirect program. The temperature of the sample was kept constant at 25 °C by means of a Lauda E300 thermostat. The weak conductivity of the  $\beta$ -CD solution was taken into account in the fitting procedure. The molar conductivity of iodide ( $\lambda(\text{I}^-) = 76.8 \text{ S cm}^2 \text{ mol}^{-1}$ )<sup>36</sup> present as the counter-ion in the solutions of the guests was kept fixed in the fitting procedure.

**Computations:** Geometry optimizations of the complexes were performed with the Gaussian 16 program package<sup>37</sup> using the CPCM(water)/B3LYP-D3(BJ)/6-31G level of theory.<sup>38</sup>

## Supplementary Information

Supplementary Information contains analytical details on binding studies of **1–3**, computational details and copies of NMR spectra.

## AUTHOR INFORMATION

### Corresponding Authors

\*E-mail: [msekutor@irb.hr](mailto:msekutor@irb.hr)

\*E-mail: [nbregovic@chem.pmf.hr](mailto:nbregovic@chem.pmf.hr)

### ORCID

M. Alešković: -

S. Roca: 0000-0001-9562-6820

R. Jozepović: -

N. Bregović: 0000-0002-7816-3323

M. Šekutor: 0000-0003-1629-3672

## Author Contributions

The manuscript was written through contributions of all authors. All authors have given approval to the final version of the manuscript.

## Notes

The authors declare no competing financial interest.

## Acknowledgements

These materials are based on work financed by the Croatian Science Foundation (HRZZ, UIP-2017-05-9653 and IP-2019-04-9560). The computations were performed on the HPC Isabella based in SRCE–University of Zagreb, University Computing Centre for computational resources.

## References

---

- <sup>1</sup> Z. Feng, T. Zhang, H. W. B. Xu, *Chem. Soc. Rev.* **2017**, *46*, 6470–6479.
- <sup>2</sup> S. Funk, J. Schatz, *J. Incl. Phenom. Macrocycl. Chem.*, **2020**, *96*, 1–27.
- <sup>3</sup> V. Balzani, M. Gómez-López, J. F. Stoddard, *Acc. Chem. Res.* **1998**, *31*, 405–414.
- <sup>4</sup> Yu Liu , Yong Chen, Heng-Yi Zhang, Handbook of Macrocyclic Supramolecular Assembly, Springer Nature Singapore Pte Ltd. 2020
- <sup>5</sup> Karsten Gloe, Macrocyclic Chemistry Current Trends and Future Perspectives, Springer, 2005.
- <sup>6</sup> G. Crini, *Chem. Rev.* **2014**, *114*, 10940–10975.
- <sup>7</sup> H. Dodziuk, *Cyclodextrins and Their Complexes. Chemistry, Analytical Methods, Applications*, WILEY–VCH, Weinheim, 2006.
- <sup>8</sup> M. V. Rekharsky, Y. Inoue, *Chem. Rev.* **1998**, *98*, 1875–1917.
- <sup>9</sup> K. A. Connors, *Chem. Rev.* **1997**, *199*, 1325–1357.

---

<sup>10</sup> S. J. Barrow, S. Kasera, M. J. Rowland, J. del Barrio, O. A. Scherman, *Chem. Rev.* **2015**, *115*, 12320–12406.

<sup>11</sup> E. Masson, X. Ling, R. Joseph, L. Kyeremeh-Mensah, X. Lu, *RSC Advances*, **2012**, *2*, 1213–1247.

<sup>12</sup> Gutsche, C. D. *Calixarenes Revisited, Monographs in Supramolecular Chemistry*; RSC, Cambridge, U.K., **1998**; Vol. 1.

<sup>13</sup> N. L. Strutt, H. Zhang, S. T. Schneebeli, J. F. Stoddart, *Acc. Chem. Res.* **2014**, *47*, 2631–2642.

<sup>14</sup> T. Ogoshi, T. Yamagishi, Y. Nakamoto, *Chem. Rev.* **2016**, *116*, 7937–8002.

<sup>15</sup> Diederich, F. *Supramolecular Cyclophane Chemistry*. In *Supramolecular Chemistry*; Balzani, V., De Cola, L., Eds.; NATO ASI Series; Springer: Dordrecht, the Netherlands, **1992**; Vol. 371; pp 119–136.

<sup>16</sup> T. Brotin, J.-P. Dutasta, *Chem. Rev.* **2009**, *109*, 88–130.

<sup>17</sup> a) F. Biedermann, V. D. Uzunova, O. A. Scherman, W. M. Nau, A. De Simone, *J. Am. Chem. Soc.* **2012**, *134*, 15318–15323. b) F. Biedermann, W. M. Nau, H.-J. Schneider, *Angew. Chem. Int. Ed.* **2014**, *53*, 2–16.

<sup>18</sup> J. W. Steed, J. L. Atwood, *Supramolecular Chemistry*, Wiley-VCH, New York, **2009**.

<sup>19</sup> J. W. Steed, D. R. Turner, K. J. Wallace, *Core concepts in supramolecular chemistry and nanochemistry*, Wiley-VCH, New York, **2007**.

<sup>20</sup> H.-J. Schneider, A. K. Yatsimirsky, *Chem. Soc. Rev.* **2008**, *37*, 263–277.

<sup>21</sup> a) R. Glaser, A. Steinberg, M. Šekutor, F. Rominger, O. Trapp, K. Mlinarić-Majerski, *Eur. J. Org. Chem.* **2011**, *2011*, 3500–3506. b) L. Cao, M. Šekutor, P.Y. Zavalij, K. Mlinarić-Majerski, R. Glaser, L. Isaacs, *Angew. Chem. Int. Ed.* **2014**, *53*, 988–993. c) M. Šekutor, K. Molčanov, L. Cao, L. Isaacs, R. Glaser, K. Mlinarić-Majerski, *Eur. J. Org. Chem.* **2014**, *2014*, 2533–2542. d) J. Hostaš, D. Sigwalt, M. Šekutor, H. Ajani, M. Dubecký, J. Řezáč, P. Y. Zavalij, L. Cao, C. Wohlschlager, K. Mlinarić-Majerski, L. Isaacs, R. Glaser, P. Hobza, *Chem. Eur. J.* **2016**, *22*, 17226–17238. e) D. Sigwalt, M. Šekutor, L. Cao, P.Y. Zavalij, J. Hostaš, H. Ajani, P. Hobza, K. Mlinarić-Majerski, R. Glaser, L. Isaacs, *J. Am. Chem. Soc.* **2017**, *139*, 3249–3258.

<sup>22</sup> L. Cao, D. Škalamera, P. Y. Zavalij, J. Hostaš, P. Hobza, K. Mlinarić-Majerski, R. Glaser, L. Isaacs, *Org. Biomol. Chem.* **2015**, *13*, 6249–6254.

<sup>23</sup> V. Rudiger, A. Eliseev, S. Simova, H.-J. Schneider, M. J. Blandamer, P. M. Cullis, A. J. Meyer, *J. Chem. Soc., Perkin Trans. 2* **1996**, 2119–2123.

<sup>24</sup> J. Carrazana, A. Jover, F. Meijide, V. H. Soto, J. V. Tato, *J. Phys. Chem. B* **2005**, *109*, 9719–9726.

<sup>25</sup> B. Zhang, R. Breslow, *J. Am. Chem. Soc.* **1993**, *115*, 9353–9354.

<sup>26</sup> M. Weickenmeier, G. Wenz, *Macromol. Rapid Commun.* **1996**, *17*, 731–736.

<sup>27</sup> Ž. Car, I. Kodrin, J. Požar, R. Ribić, D. Kovačević, V. Petrović-Peroković, *Tetrahedron* **2013**, *69*, 8051–8063.

<sup>28</sup> A. Štimac, M. Tokić, A. Ljubetić, T. Vuletić, M. Šekutor, J. Požar, K. Leko, M. Hanževački, L. Frkanec, R. Frkanec, *Org. Biomol. Chem.* **2019**, *17*, 4640–4651.

<sup>29</sup> K. Leko, M. Hanževački, Z. Brkljača, K. Pičuljan, R. Ribić, J. Požar, *Chem. Eur. J.* **2020**, *26*, 5208–5219.

<sup>30</sup> a) J. Voskuhl, M. Waller, S. Bandaru, B. A. Tkachenko, C. Fregonese, B. Wibbeling, P. R. Schreiner, B. J. Ravoo, *Org. Biomol. Chem.*, **2012**, *10*, 4524–4530. b) F. Schibilla, J. Voskuhl, N. A. Fokina, J. E. P. Dahl, P. R. Schreiner, B. J. Ravoo, *Chem. Eur. J.* **2017**, *23*, 16059–16065.

<sup>31</sup> N. A. Fokina, B. A. Tkachenko, A. Merz, M. Serafin, J. E. P. Dahl, R. M. K. Carlson, A. A. Fokin, P. R. Schreiner, *Eur. J. Org. Chem.* **2007**, 4738–4745.

<sup>32</sup> A. A. Fokin, A. Merz, N. A. Fokina, H. Schwertfeger, S. L. Liu, J. E. P. Dahl, R. K. M. Carlson, P. R. Schreiner, *Synthesis* **2009**, 909–912.

---

<sup>33</sup> M. C. Davis, D. A. Nissan, *Synth. Commun.* **2005**, *36*, 2113–2119.

<sup>34</sup> S. Liu, C. Ruspic, P. Mukhopadhyay, S. Chakrabarti, P. Y. Zavalij, L. Isaacs, *J. Am. Chem. Soc.* **2005**, *127*, 15959–15967.

<sup>35</sup> a) A. Sabatini, A. Vacca, P. Gans, *Coord. Chem. Rev.* **1992**, *120*, 389–405. b) C. Frassineti, S. Ghelli, P. Gans, A. Sabatini, M. S. Moruzzi, A. Vacca, *Anal. Biochem.* **1995**, *231*, 374–382.

<sup>36</sup> R. A. Robinson and R. H. Stokes, *Electrolyte Solutions*, Butterworths, London, 1955.

<sup>37</sup> Gaussian 16, Revision B.01, M. J. Frisch, G. W. Trucks, H. B. Schlegel, G. E. Scuseria, M. A. Robb, J. R. Cheeseman, G. Scalmani, V. Barone, G. A. Petersson, H. Nakatsuji, X. Li, M. Caricato, A. V. Marenich, J. Bloino, B. G. Janesko, R. Gomperts, B. Mennucci, H. P. Hratchian, J. V. Ortiz, A. F. Izmaylov, J. L. Sonnenberg, D. Williams-Young, F. Ding, F. Lipparini, F. Egidi, J. Goings, B. Peng, A. Petrone, T. Henderson, D. Ranasinghe, V. G. Zakrzewski, J. Gao, N. Rega, G. Zheng, W. Liang, M. Hada, M. Ehara, K. Toyota, R. Fukuda, J. Hasegawa, M. Ishida, T. Nakajima, Y. Honda, O. Kitao, H. Nakai, T. Vreven, K. Throssell, J. A. Montgomery, Jr., J. E. Peralta, F. Ogliaro, M. J. Bearpark, J. J. Heyd, E. N. Brothers, K. N. Kudin, V. N. Staroverov, T. A. Keith, R. Kobayashi, J. Normand, K. Raghavachari, A. P. Rendell, J. C. Burant, S. S. Iyengar, J. Tomasi, M. Cossi, J. M. Millam, M. Klene, C. Adamo, R. Cammi, J. W. Ochterski, R. L. Martin, K. Morokuma, O. Farkas, J. B. Foresman, and D. J. Fox, Gaussian, Inc., Wallingford CT, 2016.

<sup>38</sup> a) A. D. Becke, *J. Chem. Phys.* **1993**, *98*, 5648–5652. b) C. Lee, W. Yang, R. G. Parr, *Phys. Rev. B* **1988**, *37*, 785–789. c) S. Grimme, J. Antony, S. Ehrlich, H. Krieg, *H. J. Chem. Phys.* **2010**, *132*, 154104. d) S. Grimme, S. Ehrlich, L. Goerigk, *J. Comput. Chem.* **2011**, *32*, 1456–1465. e) V. Barone, M. Cossi, *J. Phys. Chem. A* **1998**, *102*, 1995–2001. f) M. Cossi, N. Rega, G. Scalmani, V. Barone, *J. Comp. Chem.* **2003**, *24*, 669–681.